Science of the Total Environment 683 (2019) 389–398

Contents lists available at ScienceDirect

Science of the Total Environment

journal homepage: www.elsevier.com/locate/scitotenv

Characteristics of atmospheric fungi in particle growth events along with new particle formation in the central North China Plain

Nana Luo [a,c], Wenzhong Shi [d], Chen Liang [a], Zhengqiang Li [e], Haofei Wang [e], Wenji Zhao [f], Yingjie Zhang [g], Yuying Wang [a], Zhanqing Li [b], Xing Yan [a,*]

[a] State Key Laboratory of Remote Sensing Science, College of Global Change and Earth System Science, Beijing Normal University, Beijing 100875, China
[b] Department of Atmospheric and Oceanic Sciences and ESSIC, University of Maryland, College Park, MD, USA
[c] Department of Geography, San Diego State University, 5500 Campanile Dr., San Diego, CA 92182-4493, USA
[d] Department of Land Surveying and Geo-Informatics, The Hong Kong Polytechnic University, Hong Kong, China
[e] State Environmental Protection Key Laboratory of Satellite Remote Sensing, Institute of Remote Sensing and Digital Earth, Chinese Academy of Sciences, Beijing 100101, China
[f] College of Resource Environment and Tourism, Capital Normal University, Beijing 100048, China
[g] State Key Laboratory of Atmospheric Boundary Layer Physics and Atmospheric Chemistry, Institute of Atmospheric Physics, Chinese Academy of Sciences, Beijing 100029, China

HIGHLIGHTS

- We quantified different atmospheric fungal populations sampled in Xingtai, China.
- DNA sequence-based methods were used to obtain fungal communities information.
- The characteristics of atmospheric fungi in particle growth events were investigated.

GRAPHICAL ABSTRACT

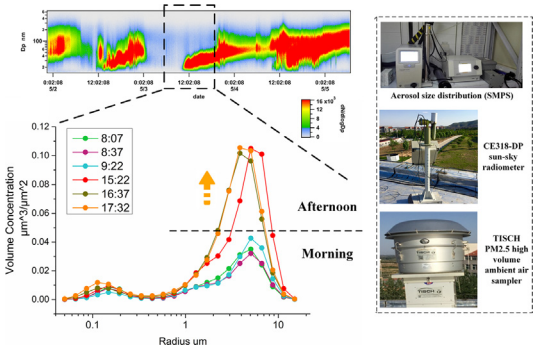

ARTICLE INFO

Article history:
Received 30 March 2019
Received in revised form 13 May 2019
Accepted 20 May 2019
Available online 21 May 2019

Editor: Jianmin Chen

Keywords:
Aerosol
Air samples
Fungi
New particle formation

ABSTRACT

The importance of fungi as cloud condensation nuclei (CCN) and ice-forming nuclei (IN) has been recognized for some researches. Particle growth along with new particle formation (NPF) play a joint role in modulating the CCN number concentration. Although fungi can accelerate the coalescence by large particles, the specific contribution and characteristics of atmospheric fungi for particle growth, especially during NPF events, is poorly understood. In this study, aerosol size distribution data and air samples were collected at Xingtai, a suburban site in the central North China Plain, from 1 May to 1 June 2016. Using DNA sequence-based methods, atmospheric fungal communities were identified and quantified. Significant differences in fungal communities between particle growth events along with new particle formation (PGE-NPF) and non-PGE-NPF events are found, especially for the *Ascomycota* and *Basidiomycota* phyla, and the *Dothideomycetes*, *Saccharomycetes*, and *Tremellomycetes* classes. At the genus level, five fungal communities were significantly different under PGE-NPF and non-PGE-NPF conditions, i.e., the *Cladosporium*, *Capnodiales*, *Mrakia*, *Saccharomycetales* and *Trichocomaceae* genera. The air mass source not only had an impact on NPF and the particle growth process, but also on the characteristics of the fungal communities. The fungal genus communities of *Cladosporium*, *Capnodiales*, *Trichocomaceae*, *Mrakia*, and *Saccharomycetales* may contribute to NPF and the particle growth process.

* Corresponding author.
E-mail address: yanxing@bnu.edu.cn (X. Yan).

https://doi.org/10.1016/j.scitotenv.2019.05.299
0048-9697/

1. Introduction

Earth's atmospheric microorganisms like fungi can influence atmospheric physics, climate, and human health (Elbert et al., 2007). The microbes can participate in long-distance transport and affect huge areas and massive numbers of people (Tang et al., 2018). Fungi are ubiquitous in the atmospheric environment and are one of the most common classes of primary biological aerosol particles (Després et al., 2012). In addition, fungi comprise 23% of the total primary emissions of organic aerosols (Heald and Spracklen, 2009).

The importance of airborne fungi is amplified in the process of cloud formation and development due to their roles as both cloud condensation (CCN) and ice nuclei (IN) (Möhler et al., 2007; Heald and Spracklen, 2009; Iannone et al., 2011). Several dicarboxylic acids have been identified as predominant constituents of organic CCN which can be efficiently transformed by fungi in the boundary layer (Yu, 2000; Ariya et al., 2002; Sun and Ariya, 2006). Laboratory studies have also indicated that certain species of fungi are highly efficient IN, such as *Fusarium* (Pouleur et al., 1992), *Isaria farinose*, and *Acremonium implicatum* (Huffman et al., 2013).

Particle growth is an important process in CCN formation because only atmospheric aerosols capable of growing to sizes of 50 nm or larger can act as CCN (Pierce et al., 2014; Sarangi et al., 2015), although smaller particles may serve under certain special circumstances (Fan et al., 2018). New particle formation (NPF) sometimes occurs during particle growth events and contributes to CCN number concentration significantly (Kuwata et al., 2008; Li et al., 2017). The NPF is defined that its particle formation rates for 3 nm typically vary from 1 to 70 cm^{-3} s^{-1} and the growth rate of new nucleated particles has been observed in the range of 1–20 nm h^{-1} (Yue et al., 2010; Yao et al., 2018; Shen et al., 2019; Lv et al., 2018). Wiedensohler et al. (2009) found that atmospheric aerosols in the growing mode contributed ~80% to the CCN number concentration on a NPF day in the North China Plain. The enhancement by NPF may differ in different regions. For example, NPF increases the CCN number concentration by 2–9 times in urban areas (Kuang et al., 2009) and by 3–10 times in coastal areas (O'Dowd, 2001).

In the particle growth process, although biological particles, such as fungi can accelerate the coalescence by large particles (Möhler et al., 2007), less is known about what specific contribution is made by atmospheric fungi to particle growth, especially on NPF day. Many studies have investigated particle growth from the chemical point of view (Zhang et al., 2011; Zhang et al., 2015), but the link between fungi and the particle growth process or NPF is not clear. A detailed investigation about the airborne fungi population and diversity during particle growth or NPF events is thus needed. Airborne fungi have been quantified using the cultivation method (Heid et al., 1996; Lau et al., 2006). However, fungi quantified by this method may not accurately reflect the true fungal species because some fungi cannot be cultured (Lang-Yona et al., 2012). The culture environment in the laboratory and the true atmosphere also differ. Others have reported limitations for culturing airborne fungi (e.g., Amann et al., 1995; Buttner et al., 1997; Hospodsky et al., 2010). DNA sequence-based methods have been proposed to

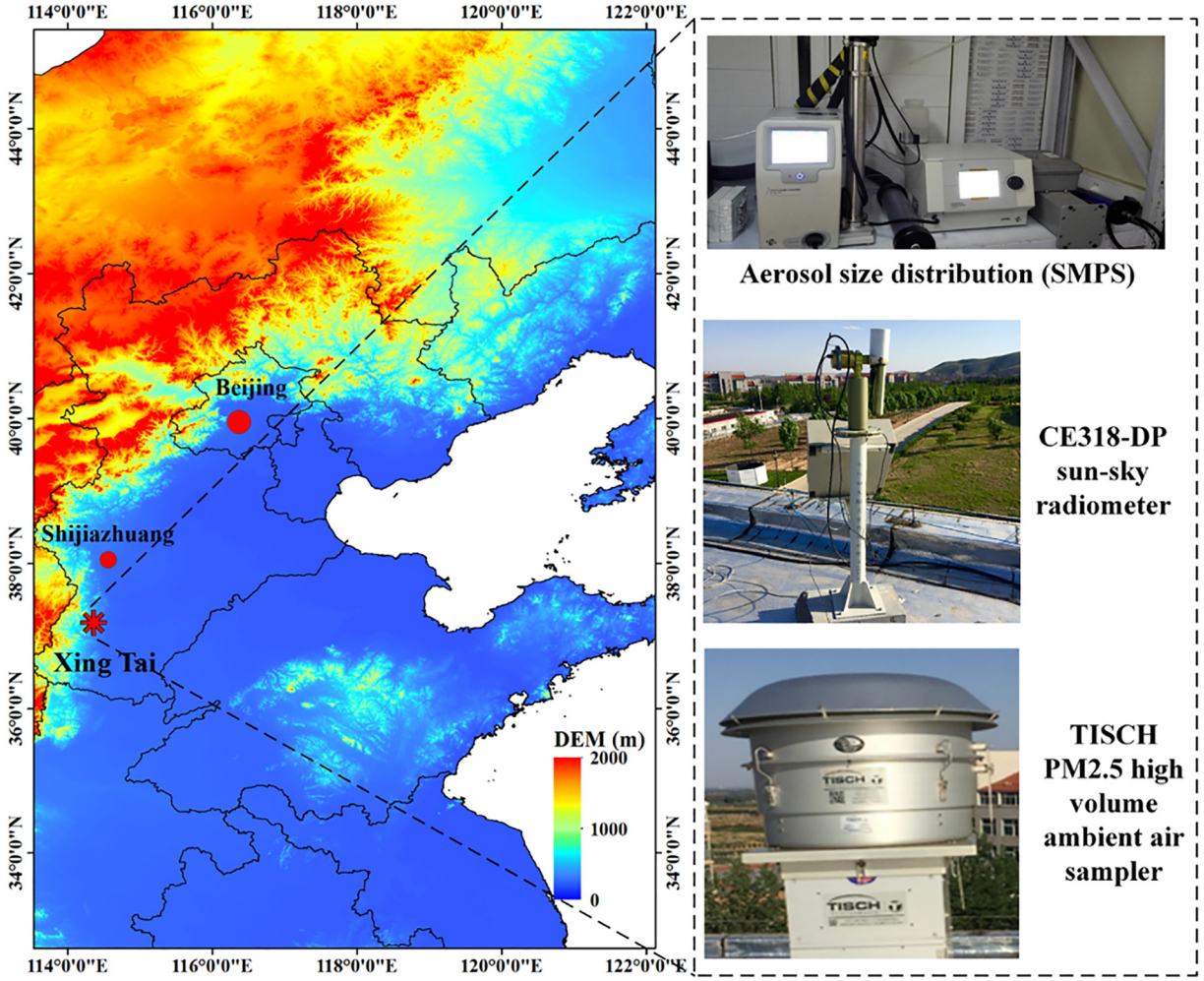

Fig. 1. Location of the sampling site (Xingtai) and instruments used in this study.

circumvent the cultivation method's limitations in detecting culturable and non-culturable atmospheric fungi (Fröhlich-Nowoisky et al., 2009; Dannemiller et al., 2014). DNA sequence-based methods can make hundreds to thousands of identifications in each sample and are useful for identifying fungal species, concentrations, and diversity (Dannemiller et al., 2014).

In this study, we quantify different atmospheric fungal populations sampled in the central North China Plain by DNA sequence-based methods. Along with aerosol particle number size distribution measurements, the goal of this study is to investigate and characterize atmospheric fungal diversity and explore possible correlations between fungal species and particle growth events on NPF days.

2. Materials and methods

2.1. Sample collection

The sampling site is Xingtai located in the central North China Plain (NCP) (Fig. 1), which is located in southern Heibei Province and to the east of the Taihang Mountains. Local industrial and domestic sources are the greatest contributors to air pollution in this study area. Air samples were taken from the roof of a two-story building at the Xingtai National Meteorological Station (37.18°N, 114.37°E) during the Aerosol Atmosphere Boundary-Layer Cloud (A^2BC) campaign. Airborne particles (particulate matter that have a diameter of <2.5 μm, or $PM_{2.5}$) were collected using a high volume air sampler (model Tish TE-6001, Tish Environment Inc., USA) which can separate particles below 2.5 μm. Ambient air was drawn at an average flow rate of 1.13 $m^3\ min^{-1}$ for 12 h during the day (7 am to 7 pm local time). Samples were collected from 1 May to 1 June 2016 (Table S1). Quartz microfiber filters (203 mm × 254 mm, WhatmanTM) were first decontaminated by baking at 500 °C then used to collect airborne particles. Each sterilized filter was packaged in sterilized aluminum foil. All collected samples were stored in a refrigerator with the temperature set at −80 °C until being used (Fröhlich-Nowoisky et al., 2009).

2.2. Aerosol size distribution measurements

Aerosol particle number size distributions (from 15 nm to 685 nm) were measured by a Scanning Mobility Particle Sizer (SMPS, model 3938, TSI Inc.) that was equipped with a differential mobility analyzer (3081L, TSI Inc.) and a condensation particle counter (3775, TSI Inc.). In addition, we also obtained aerosol size distribution data using a Cimel CE318-DP sun-sky radiometer. Sky radiance almucantar measurements at 440, 670, 870, and 1020 nm combined with aerosol optical thickness retrievals were used to retrieve aerosol size distributions based on the method developed by Dubovik and King (2000). This CE318-DP sun-sky radiometer is part of the Sun-sky radiometer Observation NETwork (SONET). Data from the SONET Xingtai site are available from the Aerosol Robotic Network (AERONET) website (https://aeronet.gsfc.nasa.gov/) (Li et al., 2016). The CE318-DP-based aerosol size distributions (Holben et al., 1998) used in this study correspond to AERONET level 1.5 data (only level 1.5 data available). The AERONET level 1.5 is the cloud-screened data, which includes two major criteria in the cloud-screening procedure and the detailed methods can be found in Smirnov et al. (2000).

2.3. DNA extraction, amplification, and sequencing

Sample filters (3/4 of the total, 721 cm^2) from each sampling day were used for DNA extraction. The filters were cut into 2 × 6 cm^2 pieces and were placed in 50-ml centrifuge tubes filled with sterilized 1× PBS buffer. The samples were then pelleted at 4 °C by centrifugation at 200*g* for 2 h. After gentle vortexing, the resuspension was filtered with a 0.2-μm Supor 200 PES Membrane Disc Filter (PALL, NY, U.S.) which was then cut into small pieces and used for DNA extraction using the MO-BIO PowerSoil DNA Isolation Kit (MOBIO Laboratories, Carlsbad, CA, USA). Each sample's DNA from three independent extractions was combined, and the amount of DNA was determined by a NanoDrop ND-1000 spectrophotometer (ThermoFisher, USA). All DNA was stored at −20 °C before further analysis.

The 18S rRNA gene (379 bp) was used as the fungal specific fragment with the primers SSU0817F (5′-TTAGCATGGAATAATRRAATAGGA-3′) and 1196R (5′-TCTGGACCTGGTGAGTTTCC-3′). Rousk et al. (2010) reported that these selected primers are fungal-specific and can target a region of the 18S rRNA gene, enabling alignment of the variables between major taxa. Polymerase chain reaction (PCR) amplification was performed in an ABI GeneAmp® 9700 (Applied Biosystems, Foster City, CA, USA). The PCR components were: 5× FastPfu Buffer (4 μl), 2.5 mM dNTPs (2 μl), forward primer (5 μM, 0.8 μl), reverse primer

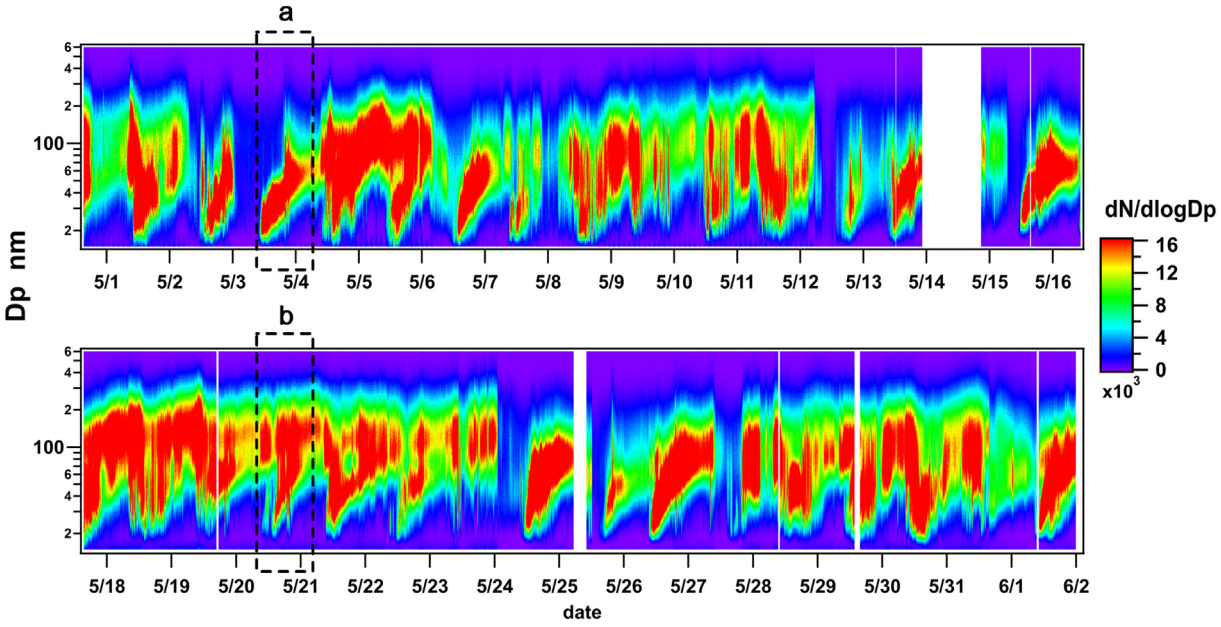

Fig. 2. Time series of particle number size distribution on (a) 3 May 2016 and (b) 20 May 2016 in Xingtai. The rectangles outlined by dashes show time periods when particle growth events along with new particle formation were observed.

(5 μM, 0.8 μl), FastPfu polymerase (0.4 μl), and template DNA (10 ng). The reaction volume was increased to 20 μl with ddH_2O. The PCR amplification used an initial denaturing step of 95 °C for 3 min, followed by 35 cycles of 95 °C for 30 s, 53 °C for 30 s, and 72 °C for 45 s, and finally an elongation step of 72 °C for 10 min.

Roch 454 high-throughput sequencing was performed in this study. Amplification products for sequencing were purified using the AxyPrep DNA Gel Extraction Kit (Axygen Biosciences, Union City, CA, USA) and quantified using QuantiFluor™-ST (Promega, Madison, WI, USA). Purified amplicons were pooled in equimolar, and paired-end reads were generated on an Illumina MiSeq platform (Majorbio Bio-Pharm Technology Co., Ltd., Shanghai, China).

2.4. Bioinformatics analysis

Fungal diversity and richness in the atmosphere were quantified based on operational taxonomic units (OTUs) with 97% sequence similarity (Liu et al., 2016). 18S rRNA gene sequences of each OTU were analyzed by a Ribosomal Database Project Classifier (http://rdp.cme.msu.edu/) against the Silva 18S rRNA database (http://www.arb-silva.de) to determine the fungal taxonomy. Rarefaction curves and Shannon-Wiener curve analyses were done to show the diversity of the samples. The Wilcoxon rank-sum test was used to check changes in fungal composition between two groups with a statistical significance $P < 0.05$. In addition, the linear discriminant analysis (LDA) effect size (LEfSe) method was used to elucidate differences in fungal taxa. This method can search the taxon for which the relative abundance is significantly different among the various populations at different taxa levels (Ling et al., 2016; Wang et al., 2012). In this study, LDA scores ≥2 were considered to be important contributors to the model and the significant alpha is 0.05.

2.5. Back trajectory analysis

To understand the source direction of the different air masses, a back trajectory analysis was done in this study. The Hybrid Single-Particle Lagrangian Integrated Trajectory (HYSPLIT) model was used to compute 72-h backward trajectories at 500 m every 12 h during the sampling period (day and night) (Wang et al., 2009). HYSPLIT is a professional model to calculate and analyze the transport and diffusion trajectories of air masses. It has been widely used in the study of atmospheric air follows in many regions. Meteorological data were obtained from the Air

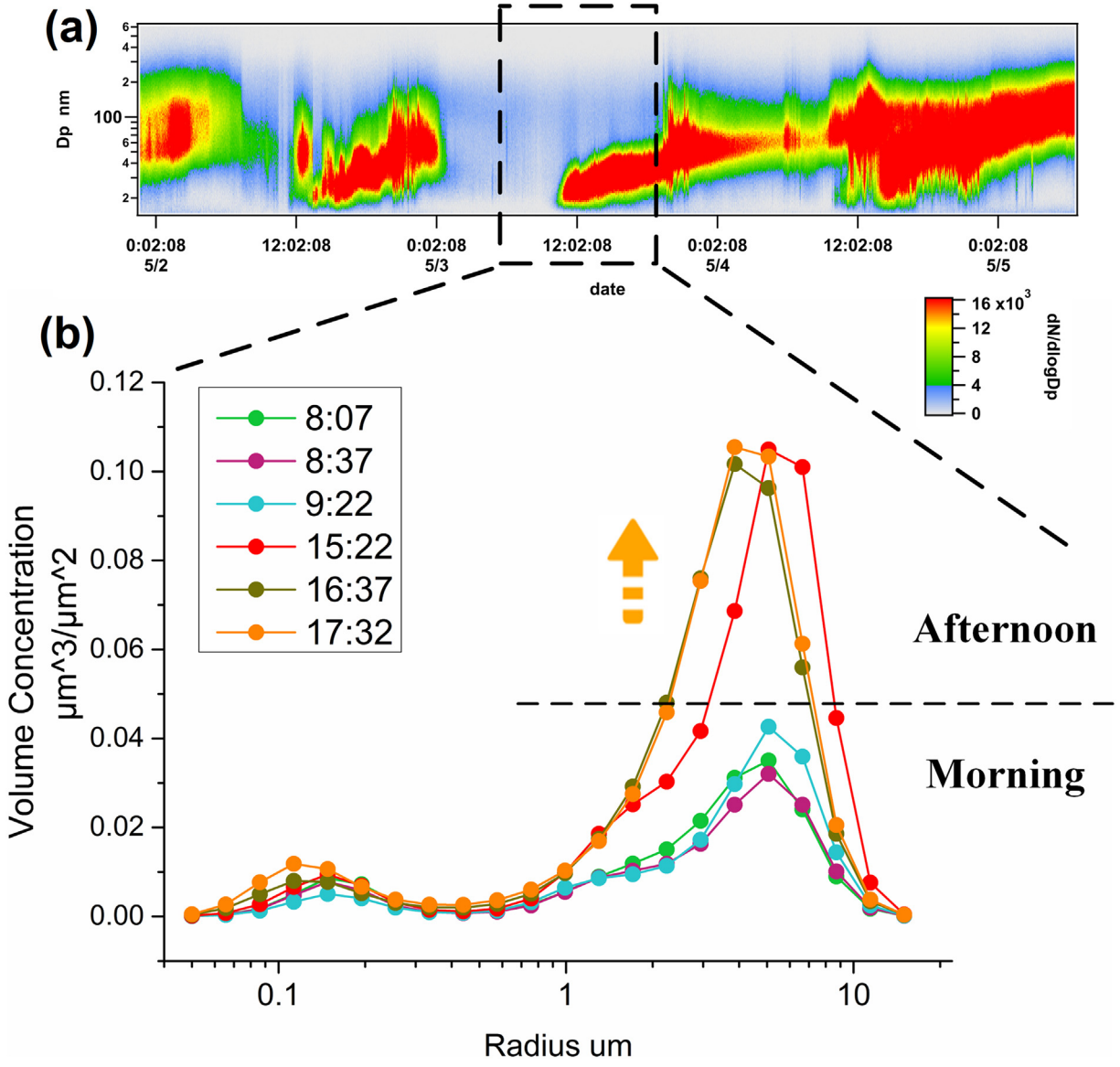

Fig. 3. (a) Particle number size distribution and (b) volume concentrations for aerosol particles on 3 May 2016 from within the rectangle outlined by dashes in (a), the time is the local time.

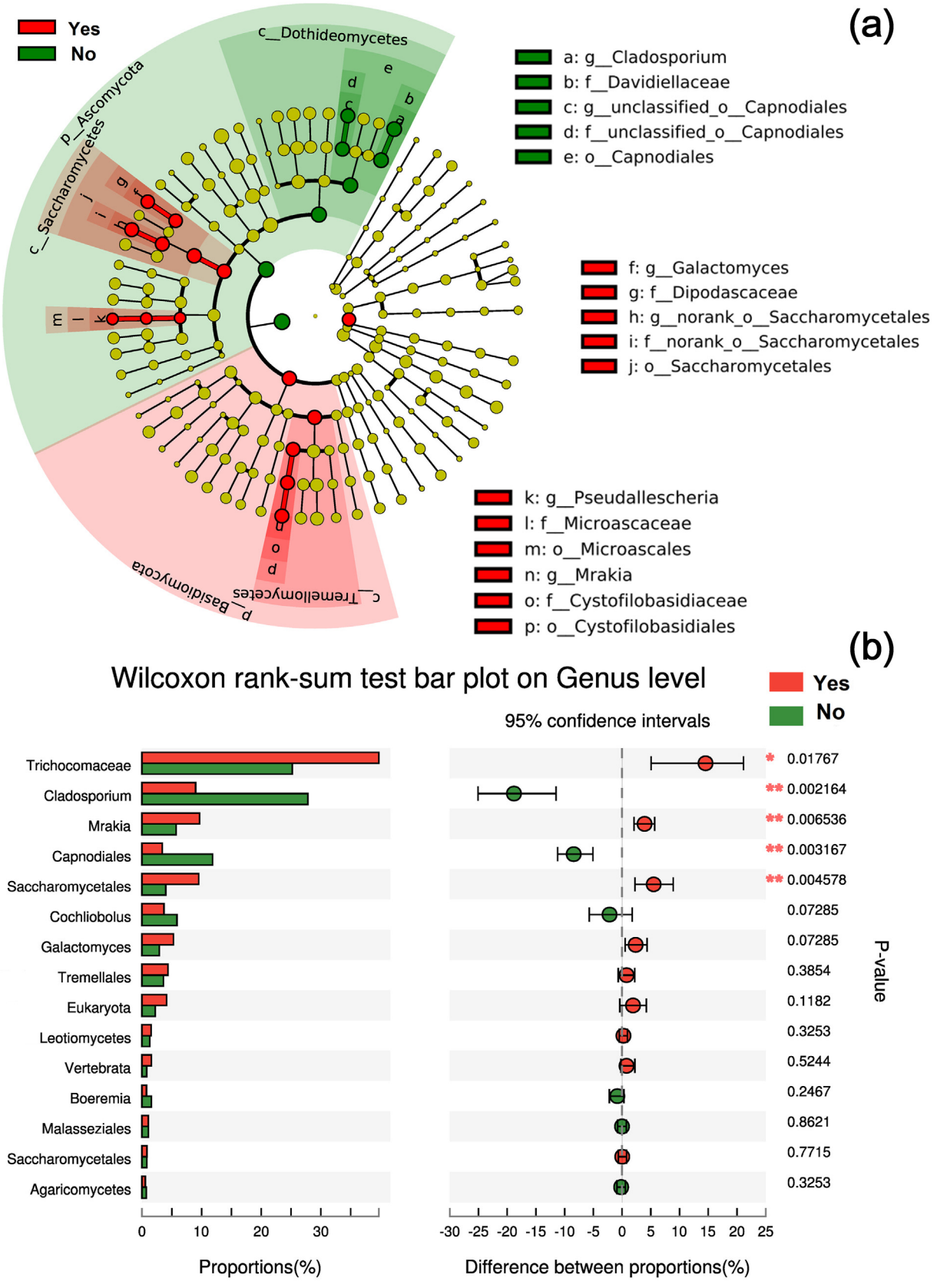

Fig. 4. (a) Taxonomic cladogram obtained by the LEfSe analysis to identify significantly different abundant taxa of fungi under PGE-NPF (Yes) and non-PGE-NPF (No) conditions. Taxa with significantly different abundances among PGE-NPF (Yes) and non-PGE-NPF (No) groups are represented by colored dots. From the center outward, they represent the kingdom, phylum, class, order, family, and genus levels. The color-shaded background represents trends of the significantly different taxa. Each colored dot has an effect size LDA score as shown in Fig. S1. (b) Wilcoxon rank-sum test for fungal taxa at the genus level in two groups: *0.01 < P ≤ 0.05, **0.01 < P ≤ 0.01. The abbreviation for Taxa levels is shown in Table S2.

Resources Laboratory website in GDAS (Global Data Assimilation System) format at a 1° spatial resolution.

3. Results and discussion

3.1. Particle size distributions and particle growth events

Fig. 2 shows the time series of particle number size distributions measured by the SMPS on 3 May and 20 May 2016. The particle number size distribution changes dramatically from day to day. Relatively high concentrations of particles in the 20–200 nm size range were seen in Xingtai during the sampling period. In addition, particle growth events along with NPF are clearly observed (Wang et al., 2018). On the NPF day, the particle number concentration between 15 and 50 nm (N_{15-50} nm) suddenly increased around 10:00 pm, and the particle growth process continued until midnight. This occurred on both clean and polluted days, e.g., on 3 May 2016 when the $PM_{2.5}$ concentration was 9.5 μg m^{-3} (Fig. 2a), and on 20 May 2016 when the $PM_{2.5}$ concentration was 75 μg m^{-3} (Fig. 2b). We further explore aerosol columnar volume size distribution data obtained by the CE318-DP sun-sky radiometer on 3 May 2016 (Fig. 3). It can be found that the CE318-DP can also capture the particle growth events. From the Fig. 3(b), we can observe clearly that the volume concentration for the coarse-mode aerosol particles have a various increase in the afternoon compared it is in the morning, this trend has a good agreement with the SMPS data (Fig. 3(a)). From integrated SMPS and CE318-DP sun-sky radiometer data, eight fungal samples were collected under particle growth events along with new particle formation (PGE-NPF) conditions and seven samples under non-PGE-NPF conditions (Table S1).

3.2. Characteristics of fungi in PGE-NPF conditions

The LEfSe analysis was used to identify fungi that differed significantly between PGE-NPF and non-PGE-NPF conditions in this study. Fig. 4a shows a cladogram representing the structure of the predominant fungi under PGE-NPF and non-PGE-NPF conditions. The LEfSe analysis revealed 23 discriminative features (LDA score > 2) at different taxon levels. There were 11 taxa in group Yes (PGE-NPF) and 5 taxa in group No (non-PGE-NPF) (Fig. 4a). The colored red and green taxa may be used as biomarkers for exploring the contribution of these species to PGE-NPF. At the genus level, *Cladosporium* and *Capnodiales* were most abundant under non-PGE-NPF conditions. These communities belong to the class of *Dothideomycetes* (c_Dothideomycetes) and the phylum of *Ascomycota* (p_Ascomycota). By contrast, although *Saccharomycetales* (g__norank_o__Saccharomycetales), *Galactomyces* (g_Galactomyces) and *Pseudoplatyophyra* (g__Pseudoplatyophyra) are also in the *Ascomycota* phylum, they belong to the class of *Saccharomycetes* (c_Saccharomycetes) and were most abundant under PGE-NPF conditions. The genus *Mrakia* (g_Mrakia), which belongs to the class of *Tremellomycetes* (c_Tremellomycetes) and the phylum of *Basidiomycota* (p__Basidiomycota), was enriched under PGE-NPF conditions as well. We further analyzed the fungal community structure at the genus level using the Wilcoxon rank-sum test which is a more strict two-tailed difference test. The bar plot on the left in Fig. 4b shows the mean relative abundance of the fungal community in two groups and the right interval plot shows differences in the fungal community at the 95% confidence level (only the top 15 most abundant genera are shown in the figure). Significant differences are seen in five fungal communities between the Yes and No groups: *Cladosporium* (P ≤ 0.01), *Capnodiales* (P ≤ 0.01), *Mrakia* (P ≤ 0.01), *Saccharomycetales* (P ≤ 0.01),

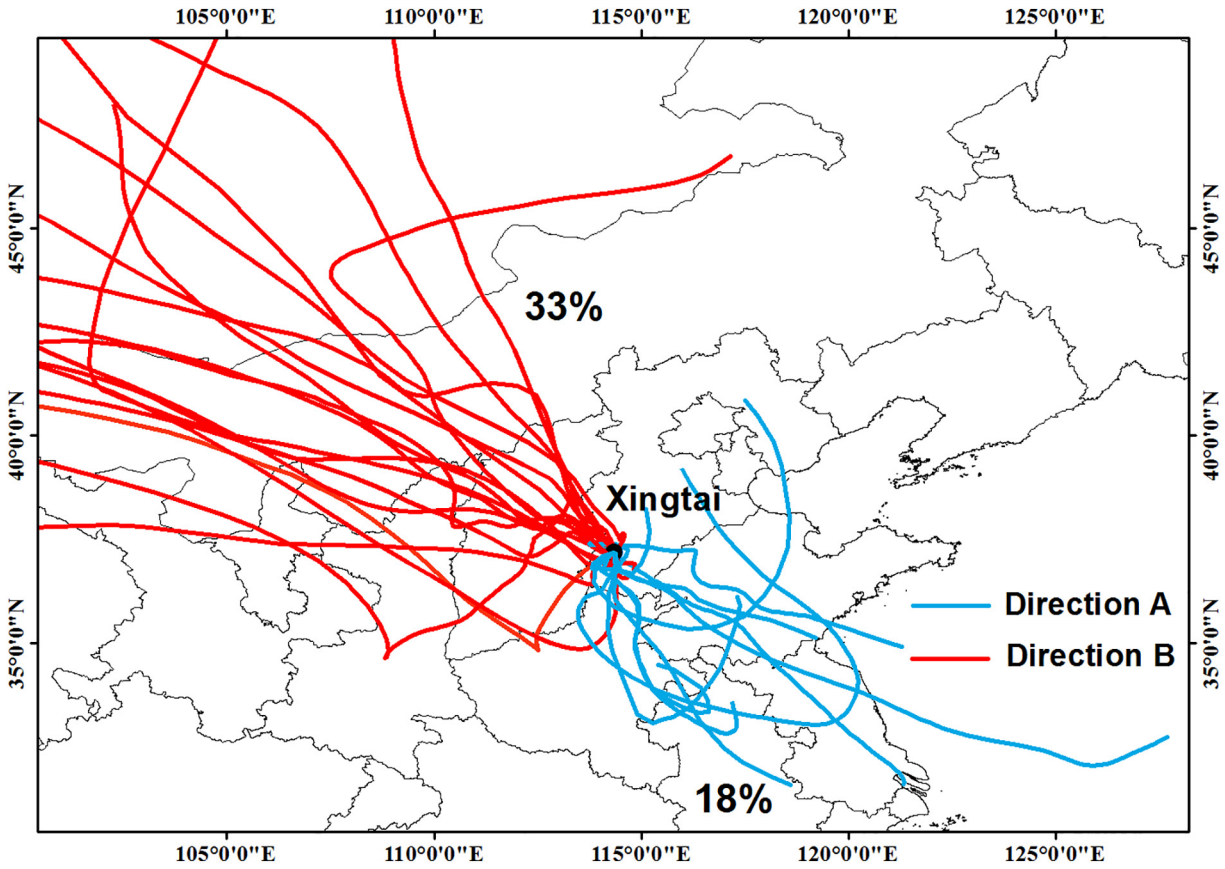

Fig. 5. HYSPLIT back trajectories at 500 m centered on Xingtai during the sampling period. Blue line: direction A represents the source of air masses from the east to Xingtai. Red line: Direction B represents the source of air masses from the west to Xingtai. (For interpretation of the references to color in this figure legend, the reader is referred to the web version of this article.)

and *Trichocomaceae* (P ≤ 0.05). *Cladosporium* and *Capnodiales* have a higher relative abundance under non-PGE-NPF conditions. The genera *Trichocomaceae*, *Mrakia*, and *Saccharomycetales* are significantly less abundant under non-PGE-NPF conditions.

3.3. Particle growth events and fungi characteristics in different air masses

Fig. 5 shows results from the HYSPLIT analysis. Based on HYSPLIT back trajectories, we classify air masses according to direction: direction A (air masses from the east to Xingtai, N = 18) and direction B (air masses from the west to Xingtai, N = 11). Air masses from the south are too few (N = 2) so are not considered here. Direction B air masses originate from Inner Mongolia and pass over mountains and through forests (Fig. 1). These are considered clean air masses. However, Direction A air masses flow across many relatively polluted urbanized and industrialized regions (Zhang et al., 2018). Integrated with SMPS data, we find that 18% of the HYSPLIT back trajectories from the direction A occur the clearly PGE-NPF, and for the direction B is 33%.

To understand the disjointed or shared fungal communities at the genus level between these two directions, a Venn diagram was developed to observe overlaps Fig. 6 shows that 42 genus communities are shared. The direction A genus community is not as rich as the direction B genus community, i.e., 6 elements as opposed to 13 elements. Rarefaction curves and Shannon-Wiener curves were then generated to enable comparisons of observed fungal community richness at the genus level between the two directions. As shown in Fig. S2a and c, all curves approach a plateau, suggesting that the sequencing dataset was large enough to retain most of the information about the fungal communities at the genus level in each sample. Mean values of the curves for all samples with standard deviation error bars are shown in Fig. S2b and d and confirms the greater richness of the genus community from direction B.

The heatmap analysis based on the fungal community at the genus level reveals that the fungal communities' relative abundances also differ between the two directions. Fig. 7a shows that the *Mrakia*, *Saccharomycetales*, and *Eukaryota* genus communities from direction A have a higher relative abundance than those from direction B. Direction A *Cladosporium* are less abundant. Fig. 7b shows results from the Wilcoxon rank-sum test. Seven genus communities are significantly different between the two directions: *Trichocomaceae* (P ≤ 0.05), *Cladosporium* (P ≤ 0.05), *Mrakia* (P ≤ 0.05), *Saccharomycetales* (P ≤ 0.05), *Capnodiales* (P ≤ 0.01), *Galactomyces* (P ≤ 0.05), and *Eukaryota* (P ≤ 0.05). Of these seven genus communities, only the relative abundances of *Cladosporium* and *Capnodiales* from direction B are greater than from direction A.

4. Discussion

In this study, we find that fungal communities have significant differences under PGE-NPF and non-PGE-NPF conditions (Fig. 4), especially at the genus levels of *Cladosporium*, *Capnodiales*, *Mrakia*, *Saccharomycetales*, and *Trichocomaceae*. Of these communities, *Cladosporium*, *Capnodiales*, and *Saccharomycetales* all belong to the phylum of *Ascomycota*. Two IN-active fungi, *Isaria farinose* and *Acremonium implicatum*, also belonging to the phylum of *Ascomycota* have been

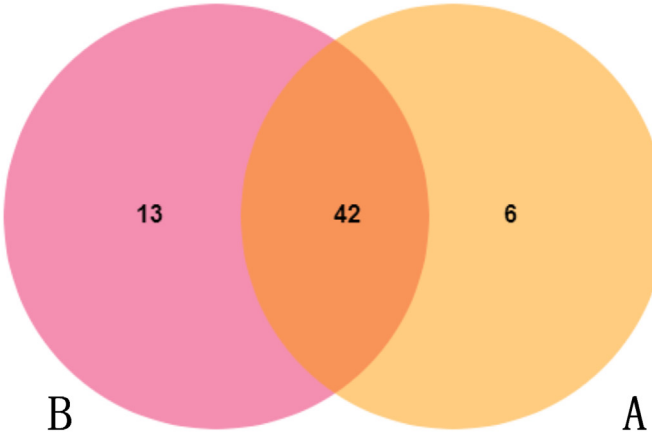

Elements only in B
Salpingoecidae
LKM15
Amoebozoa
Microstromatales
Psocoptera
Arachnida

Elements only in A
Nuclearia
Phyllopharyngea
Dothideomycetes
Embryophyta
Tremellomycetes
Ascomycota
Amoebozoa
Pseudoplatyophyra
Ochromonas
Colpodea
Telotrochidium
Fungi
Taphrina

Common elements in both		
Mrakia	Oryza	Pezizales
Hortaea	Trichocomaceae	Meria
Bensingtonia	Sporidiobolus	Hypocreales
Hemiptera	Sporidiobolales	Cochliobolus
Galactomyces	Capnodiales	Schizophyllum
Tremellales	Mycosphaerella	Sordariales
Pseudallescheria	Malasseziales	Cladosporium
Aureobasidium	Pucciniales	Boeremia
Cryptosporidium	Vertebrata	Cryptomycota
Hypocreales	Pichia	Sordariales
Chytridiomycota	Leotiomycetes	Pleosporales
Chaetothyriales	Tremellales	Saccharomycetales
Diaporthales	Agaricomycetes	Saccharomycetales
Helvella	Eukaryota	Basidiomycota

Fig. 6. The Venn diagram illustrating the overlap of fungal taxa at the genus level between directions A and B.

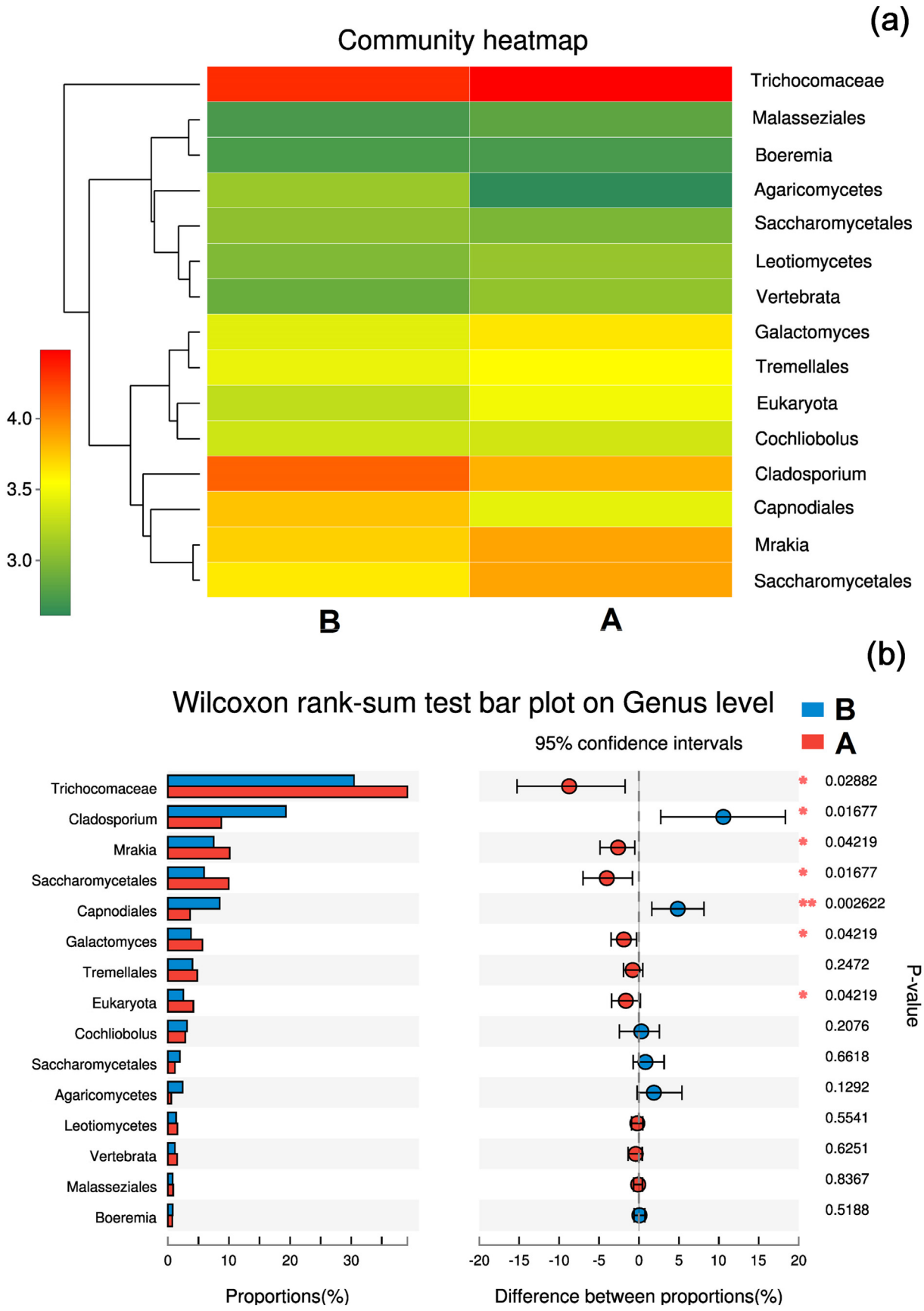

Fig. 7. (a) Heatmap of the top 15 genus communities from direction A and direction B. Colors represent log (relative abundance). (b) Wilcoxon rank-sum test for fungal communities at the genus level in two groups: *0.01 < P ≤ 0.05, **0.01 < P ≤ 0.01.

found (Huffman et al., 2013). This suggests that the phylum of *Ascomycota* plays an important role in the atmospheric nucleation and growth process. *Cladosporium* is one of most abundant types of fungal spores in the atmosphere, and its ice nucleation ability has been investigated (Iannone et al., 2011). *Cladosporium* have been frequently observed as the dominant spore near the ground (Pyrri and Kapsanaki-Gotsi, 2007; Mallo et al., 2011). In this study, we also find a high relative abundance of *Cladosporium* at Xingtai. Its mean relative abundance is ~10% under PGE-NPF conditions and 28% under non-PGE-NPF conditions. This finding suggests that in addition to its ice-nucleating ability, *Cladosporium* can also play a role in the particle growth and NPF process.

The source direction of air masses is an important factor in the particle growth and NPF process (Nilsson et al., 2001). We found that NPF events often occur when clean air flows to Xingtai from the north and the west (direction B, Fig. 5). However, this study shows that NPF also occurs when air flows in from polluted regions (direction A). This is consistent with earlier studies that reported the more frequent occurrence of NPF events in the polluted atmosphere of northern China (e.g., Wang et al., 2017). Pierce et al. (2014) have also reported the occurrence of NPF events when air flowed in from both clean and polluted regions. In addition, they revealed that NPF rates tended to be faster under polluted conditions. As shown in Fig. 7, the source direction of air masses also has a significant impact on fungal communities (Jeon et al., 2013). Seven genus communities (*Trichocomaceae*, *Cladosporium*, *Mrakia*, *Saccharomycetales*, *Capnodiales*, *Galactomyces*, and *Eukaryota*) in air masses from direction A and direction B differ significantly. Of these seven genus communities, five (*Cladosporium*, *Capnodiales*, *Mrakia*, *Saccharomycetales*, and *Trichocomaceae*) show significant differences under PGE-NPF and non-PGE-NPF conditions (Section 3.2). The richness of the genus community from direction A is less than that from direction B. Direction A air mass backward trajectories (Fig. 5) show that many air masses originated over the sea. Di Giorgio et al. (1996) have shown that fungal concentrations are lower when the wind direction is from the sea. This is because sea aerosols may have a toxic effect on atmospheric micro-organisms (Jones and Harrison, 2004).

5. Conclusions

In this study, we carried out a field experiment from 1 May to 1 June 2016 at Xingtai in the central North China Plain to investigate the characteristics of atmospheric fungi under PGE-NPF conditions. SMPS and CE318-DP sun-sky radiometer instruments were used to analyze PGE-NPF cases. DNA sequence-based methods were also used to obtain in-depth information about atmospheric fungal communities.

The LEfSe analysis shows that fungal communities under PGE-NPF and non-PGE-NPF conditions have significant differences, especially the *Ascomycota* and *Basidiomycota* phyla and the *Dothideomycetes*, *Saccharomycetes*, and *Tremellomycetes* classes. At the genus level, five genus communities show significant differences under PGE-NPF and non-PGE-NPF conditions. Under non-PGE-NPF conditions, *Cladosporium* ($P \le 0.01$) and *Capnodiales* ($P \le 0.01$) have a higher relative abundance. *Trichocomaceae* ($P \le 0.05$), *Mrakia* ($P \le 0.01$), and *Saccharomycetales* ($P \le 0.01$) are significantly less under non-PGE-NPF conditions than under PGE-NPF conditions. In the back trajectory analysis, the source of air masses had an impact on the NPF and particle growth process and the characteristics of fungal communities. PGE-NPF is often observed when clean air flows in from the west and north and it also occurs when air flows in from polluted regions to the east. Seven fungal genus communities (*Trichocomaceae*, *Cladosporium*, *Mrakia*, *Saccharomycetales*, *Capnodiales*, *Galactomyces*, and *Eukaryota*) in air masses from direction A and direction B differ significantly. Five of these genus communities show significant differences under PGE-NPF conditions.

Our results suggest that the *Cladosporium*, *Capnodiales*, *Trichocomaceae*, *Mrakia*, and *Saccharomycetales* fungal communities play an important role in the NPF and particle growth process. Although the ice-nucleating ability of *Cladosporium* is investigated, the role of other fungal communities in NPF or particle growth events is poorly understood. Further fundamental field and laboratory research is required to provide in-depth information about the impact of fungi reactions on the modification of CCN/IN capabilities, and the NPF and particle growth process. As most fungal species in the atmosphere are still unknown, DNA sequence-based methods can help to elucidate the diversity of fungi and provide realistic atmospheric fungal information (Després et al., 2012).

Acknowledgments

This work was supported by the National Key Research and Development Plan of China (2017YFC1501702), the National Natural Science Foundation of China (41801329, 91544217, 91837204), and the Fundamental Research Funds for the Central Universities.

Appendix A. Supplementary data

Supplementary data to this article can be found online at https://doi.org/10.1016/j.scitotenv.2019.05.299.

References

Amann, R.I., Ludwig, W., Schleifer, K.H., 1995. Phylogenetic identification and in situ detection of individual microbial cells without cultivation. Microbiol. Mol. Biol. Rev. 59, 143–169.
Ariya, P.A., Nepotchatykh, O., Ignatova, O., Amyot, M., 2002. Microbiological degradation of atmospheric organic compounds. Geophys. Res. Lett. 29 (34/1–34/4).
Buttner, M.P., Willeke, K., Grinshpun, S.A., 1997. In: Hurst, C.J. (Ed.), Sampling and Analysis of Airborne Microorganisms, Manual of Environmental Microbiology. ASM Press, Washington, D.C. 629–640 pp.
Dannemiller, K.C., Lang-Yona, N., Yamamoto, N., Rudich, Y., Peccia, J., 2014. Combining real-time PCR and next-generation DNA sequencing to provide quantitative comparisons of fungal aerosol populations. Atmos. Environ. 84, 113–121.
Després, V., et al., 2012. Primary biological aerosol particles in the atmosphere: a review. Tellus B Chem. Phys. Meteorol. 64 (1), 15598.
Di Giorgio, C., Krempff, A., Guiraud, H., Binder, P., Tiret, C., Dumenil, G., 1996. Atmospheric pollution by airborne microorganisms in the city of Marseilles. Atmos. Environ. 30 (1), 155–160.
Dubovik, O., King, M.D., 2000. A flexible inversion algorithm for retrieval of aerosol optical properties from Sun and sky radiance measurements. J. Geophys. Res. Atmos. 105 (D16), 20673–20696.
Elbert, W., Taylor, P.E., Andreae, M.O., Pöschl, U., 2007. Contribution of fungi to primary biogenic aerosols in the atmosphere: wet and dry discharged spores, carbohydrates, and inorganic ions. Atmos. Chem. Phys. 7 (17), 4569–4588.
Fan, J., Rosenfeld, D., Zhang, Y., Giangrande, S.E., Li, Z., et al., 2018. Substantial convection and precipitation enhancements by ultrafine aerosol particles. Science 359, 411–418. https://doi.org/10.1126/science.aan8461.
Fröhlich-Nowoisky, J., Pickersgill, D.A., Després, V.R., Pöschl, U., 2009. High diversity of fungi in air particulate matter. Proc. Natl. Acad. Sci. 106 (31), 12814–12819.
Heald, C.L., Spracklen, D.V., 2009. Atmospheric budget of primary biological aerosol particles from fungal spores. Geophys. Res. Lett. 36 (9).
Heid, C.A., Stevens, J., Livak, K.J., Williams, P.M., 1996. Real time quantitative PCR. Genome Res. 6, 986–994. https://doi.org/10.1101/gr.6.10.986.
Holben, B.N., Eck, T.F., Slutsker, I., Tanre, D., Buis, J.P., Setzer, A., Vermote, E., Reagan, J.A., Kaufman, Y., Nakajima, T., Lavenu, F., Jankowiak, I., Smirnov, A., 1998. AERONET - a federated instrument network and data archive for aerosol characterization. Rem. Sens. Environ. 66, 1–16.
Hospodsky, D., Yamamoto, N., Peccia, J., 2010. Accuracy, precision, and method detection limits of quantitative PCR for airborne bacteria and fungi. Appl. Environ. Microbiol. 76, 7004–7012. https://doi.org/10.1128/aem.01240-10.
Huffman, J.A., et al., 2013. High concentrations of biological aerosol particles and ice nuclei during and after rain. Atmos. Chem. Phys. 13 (13), 6151.
Iannone, R., Chernoff, D.I., Pringle, A., Martin, S.T., Bertram, A.K., 2011. The ice nucleation ability of one of the most abundant types of fungal spores found in the atmosphere. Atmos. Chem. Phys. 11 (3), 1191–1201.
Jeon, E.M., Kim, Y.P., Jeong, K., Kim, I.S., Eom, S.W., Choi, Y.Z., Ka, J.O., 2013. Impacts of Asian dust events on atmospheric fungal communities. Atmos. Environ. 81, 39–50.
Jones, A.M., Harrison, R.M., 2004. The effects of meteorological factors on atmospheric bioaerosol concentrations—a review. Sci. Total Environ. 326 (1–3), 151–180.
Kuang, C., McMurry, P.H., McCormick, A.V., 2009. Determination of cloud condensation nuclei production from measured new particle formation events. Geophys. Res. Lett. 36, L09822. https://doi.org/10.1029/2009GL037584.
Kuwata, M., Kondo, Y., Miyazaki, Y., Komazaki, Y., Kim, J.H., Yum, S.S., Tanimoto, H., Matsueda, H., 2008. Cloud condensation nuclei activity at Jeju Island, Korea in spring 2005. Atmos. Chem. Phys. 8, 2933–2948.
Lang-Yona, N., Dannemiller, K., Yamamoto, N., Burshtein, N., Peccia, J., Yarden, O., Rudich, Y., 2012. Annual distribution of allergenic fungal spores in atmospheric particulate

matter in the Eastern Mediterranean; a comparative study between ergosterol and quantitative PCR analysis. Atmos. Chem. Phys. 12 (5), 2681–2690.
Lau, A.P.S., Lee, A.K.Y., Chan, C.K., Fang, M., 2006. Ergosterol as a biomarker for the quantification of the fungal biomass in atmospheric aerosols. Atmos. Environ. 40, 249–259.
Li, Z., Zhang, Y., Shao, J., et al., 2016. Remote sensing of atmospheric particulate mass of dry PM2.5 near the ground: method validation using ground-based measurements. Remote Sens. Environ. 173, 59–68.
Li, Y., Zhang, F., Li, Z., Li, S., Wang, Z., Li, P., Sun, Y., Ren, J., Wang, Y., Cribb, M.C., Yuan, C., 2017. Influences of aerosol physicochemical properties and new particle formation on CCN activity from observations at a suburban site in China. Atmos. Res. 188. https://doi.org/10.1016/j.res.2017.01.009.
Ling, Z., Jin, C., Xie, T., Cheng, Y., Li, L., Wu, N., 2016. Alterations in the fecal microbiota of patients with HIV-1 infection: an observational study in a Chinese population. Sci. Rep. 6, 30673.
Liu, C., Li, H., Zhang, Y., Si, D., Chen, Q., 2016. Evolution of microbial community along with increasing solid concentration during high-solids anaerobic digestion of sewage sludge. Bioresour. Technol. 216, 87–94.
Lv, G., Sui, X., Chen, J., Jayaratne, R., Mellouki, A., 2018. Investigation of new particle formation at the summit of Mt. Tai, China. Atmos. Chem. Phys. 18 (3), 2243–2258.
Mallo, A., Nitiu, D., Gardella Sambeth, M., 2011. Airborne fungal spore content in the atmosphere of the city of La Plata, Argentina. Aerobiologia 27 (1), 77–84. https://doi.org/10.1007/s10453-10010- 19172-10450.
Möhler, O., DeMott, P.J., Vali, G., Levin, Z., 2007. Microbiology and atmospheric processes: the role of biological particles in cloud physics. Biogeosciences 4 (6), 1059–1071.
Nilsson, E.D., Paatero, J., Boy, M., 2001. Effects of air masses and synoptic weather on aerosol formation in the continental boundary layer. Tellus B 53 (4), 462–478.
O'Dowd, C.D., 2001. Biogenic coastal aerosol production and its influence on aerosol radiative properties. J. Geophys. Res. 106, 1545–1549.
Pierce, J.R., Westervelt, D.M., Atwood, S.A., Barnes, E.A., Leaitch, W.R., 2014. New-particle formation, growth and climate-relevant particle production in Egbert, Canada: analysis from 1 year of size-distribution observations. Atmos. Chem. Phys. 14 (16), 8647–8663.
Pouleur, S., Richard, C., Martin, J.H., Antoun, H.A., 1992. Ice nucleation activity in Fusarium acuminatum and Fusarium avenaceum. Appl. Environ. Microbiol. 58 (9), 2960–2964.
Pyrri, I., Kapsanaki-Gotsi, E., 2007. A comparative study on the airborne fungi in Athens, Greece, by viable and non-viable sampling methods. Aerobiologia 23, 3–15.
Rousk, J., Bååth, E., Brookes, P.C., Lauber, C.L., Lozupone, C., Caporaso, J.G., et al., 2010. Soil bacterial and fungal communities across a ph gradient in an arable soil. ISME J. 4 (10), 1340–1351.
Sarangi, B., Aggarwal, S.G., Gupta, P.K., 2015. A simplified approach to calculate particle growth rate due to self-coagulation, scavenging and condensation using SMPS measurements during a particle growth event in New Delhi. Aerosol Air Qual. Res. 15 (1), 166–179.
Shen, L., Wang, H., Yin, Y., Chen, J., Chen, K., 2019. Observation of atmospheric new particle growth events at the summit of mountain Tai (1534 m) in Central East China. Atmos. Environ. 201, 148–157.
Smirnov, A., Holben, B.N., Eck, T.F., Dubovik, O., Slutsker, I., 2000. Cloud-screening and quality control algorithms for the AERONET database. Remote Sens. Environ. 73 (3), 337–349.
Sun, J., Ariya, P.A., 2006. Atmospheric organic and bio-aerosols as cloud condensation nuclei (CCN): a review. Atmos. Environ. 40 (5), 795–820.
Tang, K., Huang, Z., Huang, J., Maki, T., Zhang, S., Ma, X., Shi, J., Bi, J., Zhou, T., Wang, G., Zhang, L., 2018. Characterization of atmospheric bioaerosols along the transport pathway of Asian dust during the Dust-Bioaerosol 2016 Campaign. Atmos. Chem. Phys. 18, 7131–7148. https://doi.org/10.5194/acp-18-7131-2018.
Wang, Y.Q., Zhang, X.Y., Draxler, R.R., 2009. TrajStat: GIS-based software that uses various trajectory statistical analysis methods to identify potential sources from long-term air pollution measurement data. Environ. Model Softw. 24 (8), 938–939.
Wang, Y., Sheng, H.F., He, Y., Wu, J.Y., Jiang, Y.X., Tam, N.F.Y., Zhou, H.W., 2012. Comparison of the levels of bacterial diversity in freshwater, intertidal wetland, and marine sediments by using millions of illumina tags. Appl. Environ. Microbiol. 78 (23), 8264–8271.
Wang, Z., Wu, Z., Yue, D., Shang, D., Guo, S., Sun, J., Ding, A., Wang, L., Jiang, J., Guo, H., 2017. New particle formation in China: current knowledge and further directions. Sci. Total Environ. 577, 258–266. https://doi.org/10.1016/j.scitotenv.2016.10.177.
Wang, Y., Li, Z., Zhang, Y., Du, W., Zhang, F., Tan, H., et al., 2018. Characterization of aerosol hygroscopicity, mixing state, and CCN activity at a suburban site in the central North China Plain. Atmos. Chem. Phys. 18 (16), 11739–11752.
Wiedensohler, A., Cheng, Y.F., Nowak, A., Wehner, B., Achtert, P., Berghof, M., Birmili, W., Rose, D., Poschl, U., Hu, M., Zhu, T., Takegawa, N., Kita, K., Kondo, Y., Lou, S.R., 2009. Rapid particle growth by secondary aerosol formation to CCN – a case study for the polluted aerosol in North-Eastern China. J. Geophys. Res. 114, D00G08. https://doi.org/10.1029/2008JD010884.
Yao, L., Garmash, O., Bianchi, F., Zheng, J., et al., 2018. Atmospheric new particle formation from sulfuric acid and amines in a Chinese megacity. Science 361 (6399), 278–281.
Yu, S.C., 2000. Review: role of organic acids formic, acetic, pyruvic and oxalic in the formation of cloud condensation nuclei CCN: a review. Atmos. Res. 53, 185–217.
Yue, D.L., Hu, M., Zhang, R.Y., Wang, Z.B., Zheng, J., Wu, Z.J., ... Zhu, T., 2010. The roles of sulfuric acid in new particle formation and growth in the mega-city of Beijing. Atmos. Chem. Phys. 10 (10), 4953–4960.
Zhang, R., Khalizov, A., Wang, L., Hu, M., Xu, W., 2011. Nucleation and growth of nanoparticles in the atmosphere. Chem. Rev. 112 (3), 1957–2011.
Zhang, R., Wang, G., Guo, S., Zamora, M.L., Ying, Q., Lin, Y., et al., 2015. Formation of urban fine particulate matter. Chem. Rev. 115 (10), 3803–3855.
Zhang, Y., Du, W., Wang, Y., Wang, Q., Wang, H., Zheng, H., et al., 2018. Aerosol chemistry and particle growth events at an urban downwind site in North China Plain. Atmos. Chem. Phys. 18 (19).